

Reactions of Boratabenzene Yttrium Complexes with KN(SiMe₃)₂: Salt Elimination and π -Ligand Displacement

Yuan Yuan, Yaofeng Chen,* Guangyu Li, and Wei Xia

State Key Laboratory of Organometallic Chemistry, Shanghai Institute of Organic Chemistry, Chinese Academy of Sciences, 354 Fenglin Road, Shanghai 200032, People's Republic of China

Received August 9, 2008

Several solvent-free boratabenzene yttrium chlorides were synthesized and structurally characterized. Their reactions with KN(SiMe₃)₂ first gave boratabenzene yttrium amides; the latter reacted further with KN(SiMe₃)₂, which results in π -ligand displacement. The boratabenzene yttrium amides showed good catalytic activities for intramolecular hydroamination.

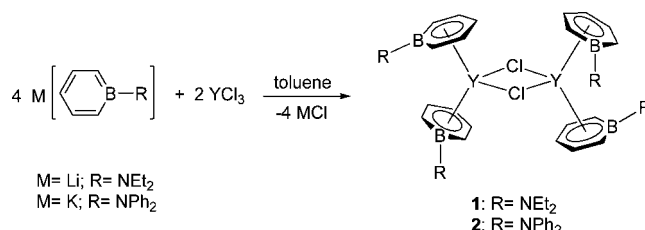
Introduction

Organometallic complexes of the rare-earth metals are of rapidly growing importance. These complexes have rich and diversified coordinating properties and reactivities¹ and have been widely used in organic² and polymer synthesis.³ The most widely investigated organometallic complexes of the rare-earth metals are those bearing Cp-type ligands. To further explore the chemistry of the rare-earth metal complexes, ancillary ligands other than Cp and Cp derivatives recently have been introduced.⁴

First reported by Herberich in 1970,⁵ boratabenzenes are heterocyclic, six- π -electron, aromatic anions that have served as versatile ligands in many transition metal complexes.⁶ Recent reports have described an increasing number of organometallic complexes of transition metals bearing boratabenzene ligands,⁷ in particular of the group 4, 6, and 8 metals. Some of these show excellent activities in the polymerization of olefins.^{7a,c,d} On the other hand, there have been only a few examples of boratabenzene derivatives of rare-earth metals, and their reactivity remains little explored.⁸

Recently, we reported several divalent lanthanide borotabenzene complexes and their reactivity in the polymerization of

Scheme 1



methyl methacrylate as well as in redox transformation with α -diimine ligands.⁹ We now have prepared several borotabenzene solvent-free yttrium(III) chlorides and have studied their reactivity toward KN(SiMe₃)₂. Herein we report these results.

Results and Discussion

Synthesis and Crystal Structures of Solvent-Free Boratabenzene Yttrium Chlorides. Salt elimination reactions^{8b} of Li[C₅H₅BN(Et)₂] and K[C₅H₅BNPh₂] with anhydrous YCl₃ in toluene provided the desired solvent-free boratabenzene yttrium chlorides [(C₅H₅BN(Et)₂)₂YCl]₂ (**1**) and [(C₅H₅BNPh₂)₂YCl]₂ (**2**) in 53% and 50% yield, respectively (Scheme 1). Both complexes were characterized by NMR (¹H, ¹³C, ¹¹B) spectroscopy and elemental analysis. A comparison of the ¹H NMR spectra of **1** and **2** with that of [(C₅H₅BCH₃)₂YCl]₂^{8b} (**3**) is instructive. The signals for 2-/6-H and 4-H in **1** (6.20 and 5.98 ppm) and **2** (6.32 and 5.81 ppm) are rather upfield in comparison to those for **3** (6.90 and 6.26 ppm), which shows that the aminoboratabenzene ligand is more electron-rich than the alkylboratabenzene ligand.

The solid-state structures of **1** and **2** were determined by X-ray crystallography (Figures 1 and 2). Complex **1** is a dimer with the Y atoms bridged by two chlorine atoms, the Y–Cl bond lengths (2.7131(13) and 2.6936(12) Å) are very similar, and the [Y1, Y1A, Cl1, Cl1A] atom grouping is a nearly perfect rhomb. The aminoboratabenzene ligands coordinate to Y atoms via the aromatic rings. This coordination mode differs from that in [(3,5-Me₂C₅H₃BNMe₂)₂ScCl]₂^{8c} where one of the aminobo-

* To whom correspondence should be addressed. E-mail: yaofchen@mail.sioc.ac.cn. Fax: (+86)21-64166128.

(1) (a) Schumann, H.; Meese-Marktscheffel, J. A.; Esser, L. *Chem. Rev.* **1995**, 95, 865. (b) Arndt, S.; Okuda, J. *Chem. Rev.* **2002**, 102, 1953. (c) Evans, W. J.; Davis, B. L. *Chem. Rev.* **2002**, 102, 2119. (d) Evans, W. J. *Inorg. Chem.* **2007**, 46, 3435.

(2) (a) Molander, G. A.; Romero, J. A. C. *Chem. Rev.* **2002**, 102, 2161. (b) Hong, S.; Marks, T. J. *Acc. Chem. Res.* **2004**, 37, 673.

(3) (a) Yasuda, H. *J. Organomet. Chem.* **2002**, 647, 128. (b) Hou, Z. M.; Wakatsuki, Y. *Coord. Chem. Rev.* **2002**, 231, 1. (c) Gromada, J.; Carpentier, J. F.; Mortreux, A. *Coord. Chem. Rev.* **2004**, 248, 397.

(4) (a) Edelmann, F. T.; Freckmann, D. M. M.; Schumann, H. *Chem. Rev.* **2002**, 102, 1851. (b) Piers, W. E.; Emslie, D. J. H. *Coord. Chem. Rev.* **2002**, 233–234, 131. (c) Gibson, V. C.; Spitzmesser, S. K. *Chem. Rev.* **2003**, 103, 283.

(5) Herberich, G. E.; Greiss, G.; Heil, H. F. *Angew. Chem., Int. Ed. Engl.* **1970**, 9, 805.

(6) Herberich, G. E.; Holger, O. *Adv. Organomet. Chem.* **1986**, 25, 199.

(7) (a) Ashe, A. J.; Al-Ahmad, S.; Fang, X. G. *J. Organomet. Chem.* **1999**, 581, 92. (b) Fu, G. C. *Adv. Organomet. Chem.* **2001**, 47, 101. (c) Bazan, G. C.; Rodriguez, G.; Ashe, A. J.; Al-Ahmad, S.; Müller, C. J. *Am. Chem. Soc.* **1996**, 118, 2291. (d) Rogers, J. S.; Bu, X. H.; Bazan, G. C. *J. Am. Chem. Soc.* **2000**, 122, 730. (e) Ashe, A. J.; Al-Ahmad, S.; Fang, X. D.; Kampf, J. W. *Organometallics* **2001**, 20, 468. (f) Herberich, G. E.; Basu Baul, T. S.; Englert, U. *Eur. J. Inorg. Chem.* **2002**, 43. (g) Auvray, N.; Basu Baul, T. S.; Braunstein, P.; Croizat, P.; Englert, U.; Herberich, G. E.; Welter, R. *Dalton Trans.* **2006**, 2950.

(8) (a) Wang, B.; Zheng, X. L.; Herberich, G. E. *Eur. J. Inorg. Chem.* **2002**, 31. (b) Zheng, X. L.; Wang, B.; Englert, U.; Herberich, G. E. *Inorg. Chem.* **2001**, 40, 3117. (c) Herberich, G. E.; Englert, U.; Fischer, A.; Ni, J. H.; Schmitz, A. *Organometallics* **1999**, 18, 5496. (d) Putzer, M. A.; Rogers, J. S.; Bazan, G. C. *J. Am. Chem. Soc.* **1999**, 121, 8112.

(9) (a) Cui, P.; Chen, Y. F.; Zeng, X. H.; Sun, J.; Li, G. Y.; Xia, W. *Organometallics* **2007**, 26, 6519. (b) Cui, P.; Chen, Y. F.; Wang, G. P.; Li, G. Y.; Xia, W. *Organometallics* **2008**, 27, 4013.

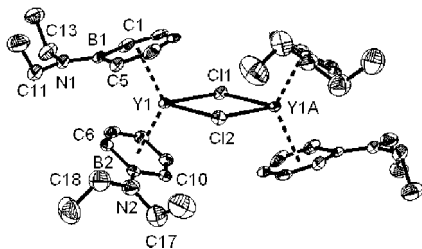


Figure 1. Molecular structure of **1** with thermal ellipsoids at the 30% probability level. Selected bond distances (Å) and angles (deg): Y1–C1 = 2.768(5), Y1–C2 = 2.658(6), Y1–C3 = 2.586(5), Y1–C4 = 2.653(5), Y1–C5 = 2.765(5), Y1–C6 = 2.692(5), Y1–C7 = 2.667(5), Y1–C8 = 2.624(5), Y1–C9 = 2.725(5), Y1–C10 = 2.783(5), Y1–Cl1 = 2.7131(13), Y1–Cl2 = 2.6936(12), B1–N1 = 1.390(7), B2–N2 = 1.408(7), Cl1–Y1–Cl2 = 79.49(4), Y1–Cl1–Y1A = 100.02(6), Y1–Cl2–Y1A = 101.01(6), Σ N1 = 359.6, Σ N2 = 359.8.

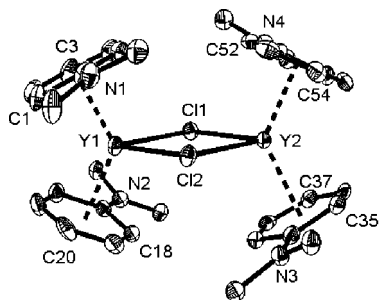


Figure 2. Molecular structure of **2** with thermal ellipsoids at the 30% probability level (the phenyl group is represented by one carbon atom, and toluene molecule in the lattice is not included). Selected bond distances (Å) and angles (deg): Y1–C1 = 2.734(8), Y1–C2 = 2.701(9), Y1–C3 = 2.661(8), Y1–C4 = 2.690(8), Y1–C5 = 2.766(8), Y1–C18 = 2.765(8), Y1–C19 = 2.709(8), Y1–C20 = 2.661(7), Y1–C21 = 2.711(8), Y1–C22 = 2.737(8), Y2–C35 = 2.731(7), Y2–C36 = 2.697(8), Y2–C37 = 2.646(7), Y2–C38 = 2.693(7), Y2–C39 = 2.769(7), Y2–C52 = 2.751(7), Y2–C53 = 2.686(7), Y2–C54 = 2.654(7), Y2–C55 = 2.711(8), Y2–C56 = 2.743(7), Y1–Cl1 = 2.673(2), Y1–Cl2 = 2.670(2), Y2–Cl1 = 2.667(2), Y2–Cl2 = 2.671(2), B1–N1 = 1.451(10), B2–N2 = 1.441(9), B3–N3 = 1.449(9), B4–N4 = 1.442(10), Cl1–Y1–Cl2 = 80.45(7), Cl1–Y2–Cl2 = 80.52(7), Y1–Cl1–Y2 = 99.54(7), Y1–Cl2–Y2 = 99.49(7), Σ N1 = 359.9; Σ N2 = 359.6; Σ N3 = 360.0; Σ N4 = 359.9.

boratabenzene ligands is coordinated through the N atom of NMe_2 substituent and the B atom and 2-C atom of the boratabenzene ring and adopting a η^3 fashion, and in $[(3,5\text{-Me}_2\text{C}_5\text{H}_3\text{BNMe}_2)_2\text{Y}(\mu\text{-Cl})_2\text{Li}]_2$,^{8a} which adopts a stepladder dimer structure with two LiCl molecules in the middle coordinated by the amino groups. The difference in coordination modes for the above three complexes can be attributed to steric effects due to the methyl substituents on the boratabenzene ring and provides examples of the diversified bonding modes of boratabenzene ligands. Slippage of Y atoms away from B atoms results in long B–Y (>3.0 Å) and Y–C(1, 5, 10) distances and in an intermediate ($\eta^5 \rightarrow \eta^3$) coordination mode, as observed in other transition metal boratabenzene complexes.⁶ The nearly trigonal-planar geometry around nitrogen atoms (Σ N1 = 359.6° and Σ N2 = 359.8°) and the rather short B–N bond distances (1.390(7) and 1.408(7) Å) indicate a fairly strong π -interaction between boron and the NEt_2 moiety.

Despite the greater steric bulk of NPh_2 substituents, complex **2** adopts a dimeric structure. The average Y–C and Y–Cl distances in **2** are 2.71 and 2.67 Å, respectively. The

sum of bond angles around the nitrogen atoms (Σ N1 = 359.9°, Σ N2 = 359.6°, Σ N3 = 360.0°, and Σ N4 = 359.9°) indicates a B–N π -interaction, but B–N bond lengths in **2** (1.451(10), 1.441(9), 1.449(9), and 1.442(10) Å) are longer than those in **1** (1.390(7) and 1.408(7) Å).

Reactions of Boratabenzene Yttrium Chlorides with $\text{KN}(\text{SiMe}_3)_2$. Reactions of $[(\text{C}_5\text{H}_5\text{BNEt}_2)_2\text{YCl}]_2$ (**1**) with $\text{KN}(\text{SiMe}_3)_2$ were studied (Scheme 2 and Figure 3). When 2 equiv of $\text{KN}(\text{SiMe}_3)_2$ in C_6D_6 was added to **1**, the ^1H NMR spectral monitoring of the reaction mixture indicated that **1** was nearly quantitatively converted into the amide $(\text{C}_5\text{H}_5\text{BNEt}_2)_2\text{YN}(\text{SiMe}_3)_2$ (**4**) within 5 min (Figure 3b). To confirm the identity of this new boratabenzene amide, **4** was synthesized by reaction of **1** with $\text{KN}(\text{SiMe}_3)_2$ in toluene and characterized by NMR (^1H , ^{13}C , ^{11}B) spectroscopy and elemental analysis. The rare-earth metal amide complexes with Cp-type ligands are usually unreactive toward an excess of $\text{KN}(\text{SiMe}_3)_2$ in the reaction mixture, but it was observed that **4** reacts further with $\text{KN}(\text{SiMe}_3)_2$. The addition of 4 equiv of $\text{KN}(\text{SiMe}_3)_2$ in C_6D_6 to **1** first generated **4**. After 1 h, a set of new signals belonging to a new boratabenzene complex were detected. The intensity of the new signals increased while those due to the amide **4** decreased with time. In addition, there was a single peak at 0.30 ppm, which also increased with time. After 24 h, the reaction was complete, and one-half of **4** was converted into the new complex **5** (Figure 3c). When more $\text{KN}(\text{SiMe}_3)_2$ (6 equiv) was used, the amide **4** was completely converted into **5** (Figure 3d). The preparation of **5** was carried out by the reaction of **1** with 6 equiv of $\text{KN}(\text{SiMe}_3)_2$ on a larger scale. The isolated **5** was characterized by NMR (^1H , ^{13}C , ^{11}B) spectroscopy and elemental analysis and shown to be a boratabenzene potassium salt, $\text{K}[(\text{C}_5\text{H}_5\text{BNEt}_2)_3\text{Y}(\text{N}(\text{SiMe}_3)_2)_3]$.¹⁰

The foregoing observations suggest the following reaction pathway: The reaction of $[(\text{C}_5\text{H}_5\text{BNEt}_2)_2\text{YCl}]_2$ with 2 equiv of $\text{KN}(\text{SiMe}_3)_2$ first generates the amide via salt elimination. When there is an excess of $\text{KN}(\text{SiMe}_3)_2$ in the reaction system, a π -ligand displacement occurs and the boratabenzene yttrium amide is converted into the diamide $(\text{C}_5\text{H}_5\text{BNEt}_2)_2\text{Y}(\text{N}(\text{SiMe}_3)_2)_2$ and $\text{K}[(\text{C}_5\text{H}_5\text{BNEt}_2)]$. The diamide immediately reacts with $\text{KN}(\text{SiMe}_3)_2$ to give the final products $\text{Y}(\text{N}(\text{SiMe}_3)_2)_3$ and $\text{K}[(\text{C}_5\text{H}_5\text{BNEt}_2)]$. The ^1H NMR monitoring of the reaction process reveals that the π -ligand displacement is much slower than the salt elimination reaction.

Reactions of $[(\text{C}_5\text{H}_5\text{BNPh}_2)_2\text{YCl}]_2$ (**2**) and $[(\text{C}_5\text{H}_5\text{BCH}_3)_2\text{YCl}]_2$ ¹¹ (**3**) with $\text{KN}(\text{SiMe}_3)_2$ also were studied. The reactions have some common features with those of **1**. When the ratio of the yttrium chloride to $\text{KN}(\text{SiMe}_3)_2$ is 1:2, the corresponding amide $(\text{C}_5\text{H}_5\text{BNPh}_2)_2\text{YN}(\text{SiMe}_3)_2$ (**6**) or $(\text{C}_5\text{H}_5\text{BCH}_3)_2\text{YN}(\text{SiMe}_3)_2$ (**7**) was the predominant product. If the amount of $\text{KN}(\text{SiMe}_3)_2$ was increased to 4 equiv, besides the amide **6** or **7**, the boratabenzene potassium salt $\text{K}[(\text{C}_5\text{H}_5\text{BNPh}_2)]$ ¹² or $\text{K}[(\text{C}_5\text{H}_5\text{BCH}_3)]$ (**8**)¹³ was formed along with $\text{Y}(\text{N}(\text{SiMe}_3)_2)_3$. When the amount of $\text{KN}(\text{SiMe}_3)_2$ was increased 6 equiv, the boratabenzene amide disappeared, and the boratabenzene potassium salt and $\text{Y}(\text{N}(\text{SiMe}_3)_2)_3$ were the only products. The amides (**6** and **7**) and the potassium salt (**8**) were prepared by the

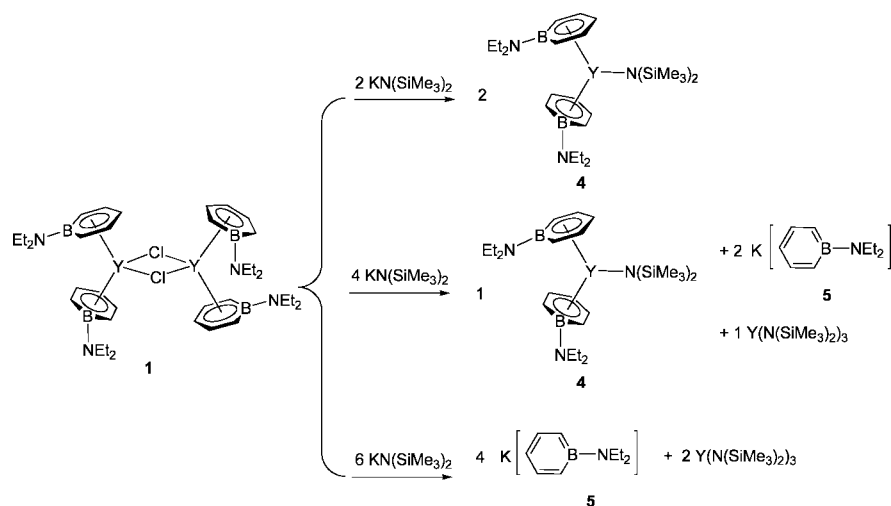
(10) Bradley, D. C.; Ghotra, J. S.; Alan Hart, F. *J. Chem. Soc., Dalton Trans.* **1973**, 1021.

(11) **3** is a known complex and was prepared as Herberich described; see ref 8b.

(12) Hoic, D. A.; DiMare, M.; Fu, G. C. *J. Am. Chem. Soc.* **1997**, *119*, 7155.

(13) Zheng, X. L.; Herberich, G. E. *Eur. J. Inorg. Chem.* **2003**, 2175.

Scheme 2



reactions of **2** and **3** with $\text{KN}(\text{SiMe}_3)_2$ in toluene and characterized by NMR (^1H , ^{13}C , ^{11}B) spectroscopy and elemental analysis. The solid-state structure of **6** was determined by single-crystal X-ray diffraction. Interestingly, the salt elimination and π -ligand displacement are greatly influenced by the B substituents. The greater steric bulk of the $-\text{NPh}_2$ substituents results in a slower salt elimination for **2** versus **1** and **3**; **4** and **6**, which with more electron-donating aminoboratabenzene ligands, undergo much slower π -ligand displacement than **7**. Although **4** and **6** both have aminoboratabenzene ligands, the π -ligand displacement occurs more easily for **6** than for **4**.

Crystal Structure of the Boratabenzene Yttrium Amide Complex. The solid-state structure of $(\text{C}_5\text{H}_5\text{BNH}_2)_2\text{YN}(\text{SiMe}_3)_2$ (**6**) was characterized by X-ray diffraction. The ORTEP figure is shown in Figure 4. The complex is a monomer and exhibits a bent metallocene-type structure wherein two NPh_2 groups point away from the metallocene wedge and are nearly perpendicular to each other. As observed in the chloride complexes, the Y atom slips away from the B atoms, with long Y–B distances (3.05 and 2.99 Å). The structural data ($\text{B1–N1} = 1.431(8)$ Å, $\text{B2–N2} = 1.448(9)$ Å; $\sum\text{N1} = 359.5^\circ$, $\sum\text{N2} = 359.8^\circ$) show that the B–N π -interaction is retained in **6**. The average Y–C

distance in **6** (2.73 Å) is close to that in **2** (2.71 Å); however the deviation in Y–C distances (up to 0.20 Å) for **6** is larger than that for **2** (0.12 Å). The most interesting structural feature is the coordination mode of the amide group. The nitrogen atom displays a trigonal-planar geometry ($\sum\text{N3} = 360.0^\circ$), and the Y–N distance of 2.199(5) Å is shorter than that in $[(\text{CH}_2)_2(\text{C}_6\text{H}_6)_2]\text{YN}(\text{SiMe}_3)_2$ (2.243(4) Å),¹⁴ indicating a fairly strong donation of the lone electron pair on nitrogen to the highly electron-deficient metal center of the boratabenzene complex. The two $\angle\text{Si–N–Y}$ angles, $107.2(2)^\circ$ and $126.8(3)^\circ$, are nonequivalent. Similar observations were made in some other rare-earth metal complexes, such as $(\text{C}_5\text{Me}_5)_2\text{YN}(\text{SiMe}_3)_2$ ($107.1(3)^\circ$ and $129.7(3)^\circ$),¹⁵ $(S)\text{[Me}_2\text{Si}(\text{C}_5\text{Me}_4)(-)\text{menthyl-Cp}]\text{SmN}(\text{SiMe}_3)_2$ ($109.0(5)^\circ$ and $121.5(4)^\circ$),¹⁶ $(R)\text{[Me}_2\text{Si}(\text{C}_5\text{Me}_4)(-)\text{menthyl-Cp}]\text{YN}(\text{SiMe}_3)_2$ ($105.9(4)^\circ$ and $123.4(4)^\circ$),¹⁶ $[\text{Me}_2\text{Si}(\text{C}_5\text{Me}_4)(\text{C}_{13}\text{H}_8)]\text{YN}(\text{SiMe}_3)_2$ ($103.6(6)^\circ$ and $132.0(7)^\circ$),¹⁷ and $[\text{Me}_2\text{Si}(\text{C}_{13}\text{H}_8)(\text{C}_5\text{H}_4)]\text{DyN}(\text{SiMe}_3)_2$ ($106.8(2)^\circ$ and $124.8(3)^\circ$).¹⁸ This was ascribed to the agostic interaction between the electron-deficient metal center and the Si–C bond. Consistent with the $\text{Y}\cdots\text{C–Si}$ agostic interaction, a close $\text{Y}\cdots\text{C37}$ contact (2.91 Å) was observed.

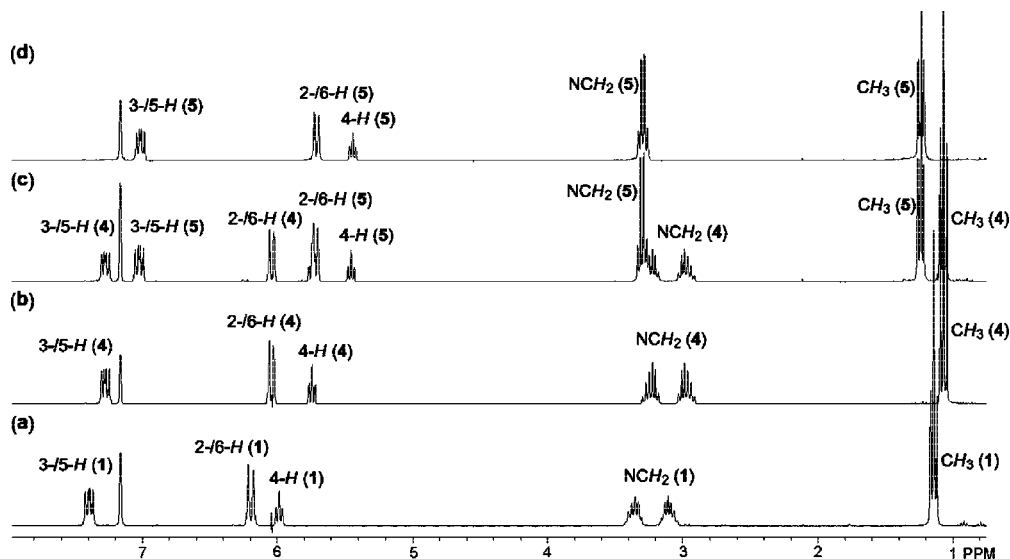


Figure 3. ^1H NMR spectra of reaction mixtures of the $[(\text{C}_5\text{H}_5\text{BNH}_2)_2\text{YCl}]_2/\text{KN}(\text{SiMe}_3)_2$ reactions at different reactant ratios: (a) $[(\text{C}_5\text{H}_5\text{BNH}_2)_2\text{YCl}]_2$; (b) $[(\text{C}_5\text{H}_5\text{BNH}_2)_2\text{YCl}]_2:\text{KN}(\text{SiMe}_3)_2 = 1:2$; (c) $[(\text{C}_5\text{H}_5\text{BNH}_2)_2\text{YCl}]_2:\text{KN}(\text{SiMe}_3)_2 = 1:4$; (d) $[(\text{C}_5\text{H}_5\text{BNH}_2)_2\text{YCl}]_2:\text{KN}(\text{SiMe}_3)_2 = 1:6$. These reactions were carried out in C_6D_6 at room temperature.

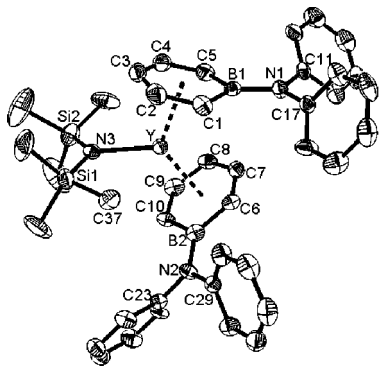


Figure 4. Molecular structure of **6** with thermal ellipsoids at the 30% probability level. Selected bond distances (Å) and angles (deg): Y–C1 = 2.827(6), Y–C2 = 2.724(7), Y–C3 = 2.665(8), Y–C4 = 2.664(7), Y–C5 = 2.756(7), Y–C6 = 2.801(6), Y–C7 = 2.693(6), Y–C8 = 2.636(7), Y–C9 = 2.744(6), Y–C10 = 2.847(6), Y–B2 = 2.991(8), Y–N3 = 2.199(5), B1–N1 = 1.431(8), B2–N2 = 1.448(9), Σ N1 = 359.5, Σ N2 = 359.8, Si1–N3–Si2 = 126.0(3), Si1–N3–Y = 107.2(2), Si2–N3–Y = 126.8(3), Σ N3 = 360.0.

Table 1. Hydroamination of 2,2-Dimethylpent-4-ene-1-amine Catalyzed by the Boratabenzene Y Amides

entry	catalyst	[cat.]/[subst.] (%)	reaction time (h)	conversion (%) ^a
1	4	5	1.0	98
2	6	5	2.9	98
3	7	5	2.4	98
4	4	3	1.5	99
5	6	3	4.7	98
6	7	3	4.7	98

^a NMR conversion determined relative to *p*-xylene internal standard.

Boratabenzene Yttrium Amide Complexes' Reactivity for Intramolecular Hydroamination. Intramolecular hydroamination offers an efficient and atom-economical method to construct nitrogen heterocycles that are important for fine chemicals and pharmaceuticals.² Various metal complexes, including those of alkali metals, early transition metals, and late transition metals, have been investigated for this transformation; the rare-earth metal complexes are among the most promising. The catalytic reactivity of the boratabenzene yttrium amide complexes in the intramolecular hydroamination was briefly tested by employing 2,2-dimethyl-1-aminopent-4-ene as the substrate (Table 1). The amides **4**, **6**, and **7** all had good activities, and the conversion of cyclization reached 98% within 3 h with 5 mol % catalyst loading. On decreasing the catalyst loading to 3 mol %, the reaction still could achieve 98% conversion within 5 h. Among these three complexes, **4** showed the highest activity, and 2,4,4-trimethylpyrrolidine was formed nearly quantitatively within 1.5 h even with 3 mol % catalyst loading, which is comparable to the most active Cp-type yttrium complexes.² As the overall activity of the complex toward

hydroamination reaction is effected by many factors, and some of these have opposite effects on different steps involved, so far it has not been possible to establish a relationship between the steric and electronic properties of these boratabenzene complexes with their activities.

In summary, salt elimination reactions of Li[C₅H₅BN(Et)₂] and K[C₅H₅BNPh₂] with anhydrous YCl₃ in toluene provided solvent-free boratabenzene yttrium chlorides [(C₅H₅BN(Et)₂)₂YCl]₂ and [(C₅H₅BNPh₂)₂YCl]₂. Both complexes adopt a dimeric structure, and the aminoboratabenzene ligands are coordinated through the aromatic rings. The boratabenzene–Y distances are longer than the Cp–Y distances. Reactions of boratabenzene yttrium chlorides with KN(SiMe₃)₂ first gave boratabenzene yttrium amides via salt elimination. The boratabenzene yttrium amides produced reacted further with KN(SiMe₃)₂ to cause π -ligand displacement and generate potassium salts of boratabenzene ligands. The π -ligand displacement is greatly influenced by the B substituents and decreases in the order –Me \gg –NPh₂ > –NEt₂. The boratabenzene yttrium amides showed good catalytic activities for the intramolecular hydroamination of 2,2-dimethyl-1-aminopent-4-ene.

Experimental Section

General Procedures. All operations were carried out under an atmosphere of argon using standard Schlenk techniques or in a nitrogen-filled glovebox. THF was distilled from Na-benzophenone ketyl. Toluene, hexane, C₆D₆, and THF-*d*₈ were dried over Na/K alloy, distilled under vacuum, and stored in the glovebox. CDCl₃ was degassed and dried over 4 Å molecular sieves. Anhydrous YCl₃ was prepared from Y₂O₃ and HCl according to the standard procedure.¹⁹ K[C₅H₅BN(C₆H₅)₂] was prepared by the method reported by Fu.¹² [(C₅H₅BCH₃)₂YCl]₂ (**3**) was synthesized following the procedure reported by Herberich.^{8b} KN(SiMe₃)₂²⁰ and 2,2-dimethyl-1-aminopent-4-ene²¹ were synthesized according to literature procedures, and 2,2-dimethyl-1-aminopent-4-ene was dried over CaH₂ for 1 day and distilled under vacuum prior to use. ¹H and ¹³C NMR spectra were recorded on a Varian Mercury 300 MHz spectrometer at 300 and 75 MHz, respectively. ¹¹B NMR spectra were recorded on a Bruker DXP 400 MHz spectrometer at 128 MHz. All chemical shifts were reported in δ units with references to the residual solvent resonance of the deuterated solvents for proton and carbon chemical shifts, and to external BF₃·OEt₂ for boron chemical shifts. Elemental analysis was performed by the Analytical Laboratory of Shanghai Institute of Organic Chemistry. Melting points of the complexes were determined on a SWG X-4 digital melting point apparatus in a sealed capillary and are uncorrected.

Synthesis of (C₅H₅BN(Et)₂)Li. C₅H₅BPMe₃ (2.30 g, 15.1 mmol) and LiNEt₂ (1.21 g, 15.3 mmol) were mixed in 35 mL of THF at 0 °C under stirring, and the reaction mixture was warmed to room temperature and stirred for 11 h. The precipitate was removed by centrifugation. Evaporation of the red solution in vacuo provided a brown oil, to which 4 mL of toluene was added to give a pale yellow solid. The latter was washed with 3 mL of toluene and 10 mL of hexane and dried under vacuum to yield the desired complex as a white solid (1.81 g, 77% yield). ¹H NMR (300 MHz, THF-*d*₈, 25 °C): δ (ppm) 7.0 (dd, *J* = 9.3 Hz, *J* = 6.9 Hz, 2H, 3-/5-*H*), 5.59 (d, *J* = 9.9 Hz, 2H, 2-/6-*H*), 5.43 (t, *J* = 6.9 Hz, 1H, 4-*H*), 3.07 (q, *J* = 6.9 Hz, 4H, NCH₂), 1.00 (t, *J* = 6.9 Hz, 6H, CH₃).

(19) Taylor, M. D. *Chem. Rev.* **1962**, 62, 503.

(20) Amonoo-Neizer, E. H.; Shaw, R. A.; Skovlin, D. O.; Smith, B. C. *J. Chem. Soc.* **1965**, 2997.

(21) (a) Tamaru, Y.; Hojo, M.; Higashimura, H.; Yoshida, Z. *J. Am. Chem. Soc.* **1988**, 110, 3994. (b) Gagné, M. R.; Stern, C. L.; Marks, T. J. *J. Am. Chem. Soc.* **1992**, 114, 275.

(14) Zhou, S. L.; Wang, S. W.; Yang, G. S.; Li, Q. H.; Zhang, L. J.; Yao, Z. J.; Zhou, Z. K.; Song, H. B. *Organometallics*. **2007**, 26, 3755.

(15) den Haan, K. H.; de Boer, J. L.; Teuben, J. H. *Organometallics*. **1986**, 5, 1726.

(16) Giardello, M. A.; Conticello, V. P.; Brard, L.; Sabat, M.; Rheingold, A. L.; Stern, C. L.; Marks, T. J. *J. Am. Chem. Soc.* **1994**, 116, 10212.

(17) Lee, M. H.; Hwang, J.-W.; Kim, Y.; Kim, J.; Han, Y.; Do, Y. *Organometallics* **1999**, 18, 5124.

(18) Qian, C. T.; Nie, W. L.; Sun, J. *Organometallics*. **2000**, 19, 4134.

^{13}C NMR (75 MHz, $\text{THF-}d_8$, 25 °C): δ (ppm) 134.4 (3-/5-C), 110.5 (2-/6-C), 99.1 (4-C), 43.9 (CH_2), 16.3 (CH_3). ^{11}B NMR (128 MHz, $\text{THF-}d_8$, 25 °C): δ (ppm) 30.9.

Synthesis of $[(\text{C}_5\text{H}_5\text{BNET}_2)_2\text{YCl}]_2$ (1). Anhydrous YCl_3 (970 mg, 4.97 mmol) and $\text{Li}[\text{C}_5\text{H}_5\text{BNET}_2]$ (1.54 g, 9.94 mmol) were mixed in 100 mL of toluene, and the reaction mixture was stirred for 3 days at 110 °C. The precipitate was removed by centrifugation, and the clear yellow solution was concentrated to about 2 mL in vacuo to give **1** as a yellow crystalline solid (1.10 g, 53% yield). Single crystals suitable for X-ray diffraction analysis were obtained from hexane solution. Mp: 132–135 °C without decomposition. ^1H NMR (300 MHz, C_6D_6 , 25 °C): δ (ppm) 7.39 (dd, $J = 11.1$ Hz, $J = 6.9$ Hz, 8H, 3-/5-*H*), 6.20 (d, $J = 10.5$ Hz, 8H, 2-/6-*H*), 5.98 (t, $J = 6.9$ Hz, 4H, 4-*H*), 3.35 (m, 8H, NCH_2), 3.11 (m, 8H, NC H_2), 1.14 (t, $J = 6.9$ Hz, 24H, CH_3). ^1H NMR (300 MHz, CDCl_3 , 25 °C): δ (ppm) 7.31 (dd, $J = 11.1$ Hz, $J = 6.8$ Hz, 8H, 3-/5-*H*), 6.05 (d, $J = 10.2$ Hz, 8H, 2-/6-*H*), 5.93 (t, $J = 6.5$ Hz, 4H, 4-*H*), 3.31 (m, 8H, NCH_2), 3.12 (m, 8H, NC H_2), 1.13 (t, $J = 6.9$ Hz, 24H, CH_3). ^{13}C NMR (75 MHz, CDCl_3 , 25 °C): δ (ppm) 142.5 (3-/5-C), 116.2 (2-/6-C), 101.0 (4-C), 42.3 (NCH_2), 15.7 (CH_3). ^{11}B NMR (128 MHz, CDCl_3 , 25 °C): δ (ppm) 31.8. Anal. Calcd (%) for $\text{C}_{36}\text{H}_{60}\text{B}_4\text{Cl}_2\text{N}_4\text{Y}_2$: C 51.42, H 7.19, N 6.66. Found: C 50.63, H 7.12, N 6.70.

Synthesis of $[(\text{C}_5\text{H}_5\text{BNPh}_2)_2\text{YCl}]_2$ (2). Following the procedure described for **1**, reaction of anhydrous YCl_3 (351 mg, 1.80 mmol) and $\text{K}[\text{C}_5\text{H}_5\text{BNPh}_2]$ (1.02 g, 3.60 mmol) in 65 mL of toluene gave **2** as a yellow crystalline solid (553 mg, 50% yield). Single crystals suitable for X-ray diffraction analysis were obtained from a toluene solution. Mp: 279–281 °C without decomposition. ^1H NMR (300 MHz, C_6D_6 , 25 °C): δ (ppm) 7.19–7.25 (m, 32H, Ph-*H*), 7.00–7.05 (m, 8H, Ph-*H*), 6.73 (dd, $J = 10.8$ Hz, $J = 6.9$ Hz, 8H, 3-/5-*H*), 6.32 (d, $J = 11.1$ Hz, 8H, 2-/6-*H*), 5.81 (t, $J = 6.9$ Hz, 4H, 4-*H*). ^1H NMR (300 MHz, CDCl_3 , 25 °C): δ (ppm) 7.34 (t, $J = 7.8$ Hz, 16H, Ph-*H*), 7.15 (t, $J = 7.2$ Hz, 8H, Ph-*H*), 7.07 (d, $J = 7.8$ Hz, 16H, Ph-*H*), 6.82 (dd, $J = 10.8$ Hz, $J = 7.2$ Hz, 8H, 3-/5-*H*), 6.11 (d, $J = 11.1$ Hz, 8H, 2-/6-*H*), 5.76 (t, $J = 6.9$ Hz, 4H, 4-*H*). ^{13}C NMR (75 MHz, CDCl_3 , 25 °C): δ (ppm) 149.3 (Ph-C), 142.6 (3-/5-C), 128.8 (Ph-C), 127.4 (Ph-C), 123.8 (Ph-C), 119.9 (2-/6-C), 103.6 (4-C). ^{11}B NMR (128 MHz, CDCl_3 , 25 °C): δ (ppm) 34.4. Anal. Calcd (%) for $\text{C}_{68}\text{H}_{60}\text{B}_4\text{Cl}_2\text{N}_4\text{Y}_2$: C 66.66, H 4.94, N 4.57. Found: C 66.58, H 5.30, N 4.36.

Reaction of $[(\text{C}_5\text{H}_5\text{BNET}_2)_2\text{YCl}]_2$ (1) with $\text{KN}(\text{SiMe}_3)_2$. (a) Reaction of **1** with 2 equiv of $\text{KN}(\text{SiMe}_3)_2$: A solution of $\text{KN}(\text{SiMe}_3)_2$ (5.7 mg, 0.028 mmol) in 0.4 mL of C_6D_6 was added to **1** (11.8 mg, 0.014 mmol) in 0.2 mL of C_6D_6 . The reaction mixture was immediately transferred into a NMR tube, and a ^1H NMR spectrum was recorded after 5 min. The spectrum showed the disappearance of **1** and the formation of $(\text{C}_5\text{H}_5\text{BNET}_2)_2\text{YN}(\text{SiMe}_3)_2$ (**4**).

(b) Reaction of **1** with 4 equiv of $\text{KN}(\text{SiMe}_3)_2$: The procedure described for (a) was used, but with $\text{KN}(\text{SiMe}_3)_2$ (9.5 mg, 0.048 mmol) and **1** (10.2 mg, 0.012 mmol). The reaction first provided **4**, and the formation of $\text{K}[\text{C}_5\text{H}_5\text{BNET}_2]$ (**5**) and $\text{Y}(\text{N}(\text{SiMe}_3)_2)_3$ was detected after an hour. The quantity of **5** and $\text{Y}(\text{N}(\text{SiMe}_3)_2)_3$ increased with time, while that of **4** decreased. After 24 h, the reaction was complete and one-half of **4** was converted into **5**.

(c) Reaction of **1** with 6 equiv of $\text{KN}(\text{SiMe}_3)_2$: The procedure described for (a) was used, but with $\text{KN}(\text{SiMe}_3)_2$ (14.2 mg, 0.072 mmol) and **1** (10.2 mg, 0.012 mmol). The reaction process was similar to that of (b). The quantity of **5** and $\text{Y}(\text{N}(\text{SiMe}_3)_2)_3$ increased with time, and **4** had disappeared when the reaction was complete. A pure sample of **5** was prepared and isolated as follows: A solution of $\text{KN}(\text{SiMe}_3)_2$ (42.7 mg, 0.214 mmol) in 2 mL of toluene was added to **1** (30 mg, 0.036 mmol) in 1.5 mL of toluene, and the reaction mixture was stirred for 2 days at room temperature. Evaporation of the reaction mixture in vacuo provided a pale yellow solid. The solid was washed by 3×1.5 mL of hexane to give **5** as

a pale yellow solid (26 mg, 97% yield). ^1H NMR (300 MHz, C_6D_6 , 25 °C): δ (ppm) 6.99 (dd, $J = 10.2$ Hz, $J = 6.6$ Hz, 2H, 3-/5-*H*), 5.70 (d, $J = 10.2$ Hz, 2H, 2-/6-*H*), 5.42 (t, $J = 6.6$ Hz, 1H, 4-*H*), 3.28 (m, $J = 6.9$ Hz, 4H, NCH_2), 1.22 (t, $J = 6.9$ Hz, 6H, CH_3). ^{13}C NMR (75 MHz, C_6D_6 , 25 °C): δ (ppm) 135.9 (3-/5-C), 111.9 (2-/6-C), 100.9 (4-C), 43.2 (NCH_2), 16.4 (CH_3). ^{11}B NMR (128 MHz, C_6D_6 , 25 °C): δ (ppm) 31.3. Removal of the solvent of the hexane extract yielded $\text{Y}(\text{N}(\text{SiMe}_3)_2)_3$ as a white solid. ^1H NMR (300 MHz, C_6D_6 , 25 °C): δ (ppm) 0.30. ^{13}C NMR (75 MHz, C_6D_6 , 25 °C): δ (ppm) 4.29. Anal. Calcd (%) for $\text{C}_9\text{H}_{15}\text{BNK}$: C, 57.76; H, 8.08; N, 7.48. Found: C, 57.65; H, 8.59; N, 7.78.

Synthesis of $(\text{C}_5\text{H}_5\text{BNET}_2)_2\text{YN}(\text{SiMe}_3)_2$ (4). A toluene solution of $\text{KN}(\text{SiMe}_3)_2$ (81.6 mg, 0.409 mmol) in 3 mL of toluene was added to **1** (172 mg, 0.204 mmol) in 3 mL of toluene. After stirring for 40 min at room temperature, the reaction mixture was filtered. Evaporation of the yellow filtrate in vacuo left a yellow oil, which was extracted with 2×2 mL of hexane. Removal of the solvent of the extract gave **4** as a yellow oil (198 mg, 89% yield). ^1H NMR (300 MHz, C_6D_6 , 25 °C): δ (ppm) 7.27 (dd, $J = 11.1$ Hz, $J = 6.6$ Hz, 4H, 3-/5-*H*), 6.04 (d, $J = 9.9$ Hz, 4H, 2-/6-*H*), 5.74 (t, $J = 6.6$ Hz, 2H, 4-*H*), 3.22 (m, 4H, NCH_2), 2.98 (m, 4H, NCH_2), 1.07 (t, $J = 6.9$ Hz, 12H, CH_3), 0.16 (s, 18H, $\text{Si}(\text{CH}_3)_3$). ^{13}C NMR (75 MHz, C_6D_6 , 25 °C): δ (ppm) 142.4 (3-/5-C), 117.2 (2-/6-C), 101.8 (4-C), 42.9 (NCH_2), 15.8 (CH_3), 3.3 ($\text{Si}(\text{CH}_3)_3$). ^{11}B NMR (128 MHz, C_6D_6 , 25 °C): δ (ppm) 32.4. Anal. Calcd (%) for $\text{C}_{24}\text{H}_{48}\text{B}_2\text{N}_3\text{Si}_2\text{Y}$: C, 52.86; H, 8.87; N, 7.71. Found: C, 52.98; H, 8.29; N, 7.66.

Reaction of $[(\text{C}_5\text{H}_5\text{BNPh}_2)_2\text{YCl}]_2$ (2) with $\text{KN}(\text{SiMe}_3)_2$. The ^1H NMR investigation procedure is similar to that for $[(\text{C}_5\text{H}_5\text{BNET}_2)_2\text{YCl}]_2$, but with $[(\text{C}_5\text{H}_5\text{BNPh}_2)_2\text{YCl}]_2$. $\text{K}[\text{C}_5\text{H}_5\text{BNPh}_2]$ was isolated and identified as follows: A solution of $\text{KN}(\text{SiMe}_3)_2$ (14.6 mg, 0.0732 mmol) in 0.5 mL of C_6D_6 was added to **2** (15 mg, 0.0122 mmol) in 0.3 mL of C_6D_6 . After stirring for 10 h at room temperature, the pale yellow precipitate was separated, washed with 0.3 mL of C_6D_6 , and dried in vacuo. The ^1H NMR spectrum of the above precipitate in $\text{THF-}d_8$ is the same as that of the $\text{K}[\text{C}_5\text{H}_5\text{BNPh}_2]$ prepared from the reaction of $\text{C}_5\text{H}_5\text{BPM}_3$ with KNPh_2 . ^1H NMR (300 MHz, $\text{THF-}d_8$, 25 °C): δ (ppm) 7.12–7.15 (m, 4H, Ph-*H*), 6.96–7.04 (m, 6H, Ph-*H* and 3-/5-*H*), 6.68 (t, $J = 6.9$ Hz, 2H, Ph-*H*), 5.97 (d, $J = 10.5$ Hz, 2H, 2-/6-*H*), 5.70 (t, $J = 6.9$ Hz, 1H, 4-*H*).

Synthesis of $(\text{C}_5\text{H}_5\text{BNPh}_2)_2\text{YN}(\text{SiMe}_3)_2$ (6). A solution of $\text{KN}(\text{SiMe}_3)_2$ (78.6 mg, 0.394 mmol) in 3 mL of toluene was added to **2** (241 mg, 0.197 mmol) in 4 mL of toluene. After stirring for 10 h at room temperature, the reaction mixture was filtered. Evaporation of the yellow solution in vacuo gave a yellow oil, which was extracted by 5×4 mL of hexane. The volume of the extract was then concentrated to approximately 4 mL to give **6** as yellow crystals (95 mg, 33% yield). Single crystals suitable for X-ray diffraction analysis were obtained from a hexane solution. Mp: 174–176 °C without decomposition. ^1H NMR (300 MHz, C_6D_6 , 25 °C): δ (ppm) 7.28 (dd, $J = 10.8$ Hz, $J = 6.6$ Hz, 4H, 3-/5-*H*), 7.24–7.13 (m, 16H, Ph-*H*), 6.96 (t, $J = 7.2$ Hz, 4H, Ph-*H*), 6.41 (d, $J = 10.2$ Hz, 4H, 2-/6-*H*), 5.93 (t, $J = 6.6$ Hz, 2H, 4-*H*), 0.05 (s, 18H, $\text{Si}(\text{CH}_3)_3$). ^{13}C NMR (75 MHz, C_6D_6 , 25 °C): δ (ppm) 150.1 (Ph-C), 142.3 (3-/5-C), 129.4 (Ph-C), 127.3 (Ph-C), 123.8 (Ph-C), 120.7 (2-/6-C), 105.0 (4-C), 3.1 ($\text{Si}(\text{CH}_3)_3$). ^{11}B NMR (128 MHz, C_6D_6 , 25 °C): δ (ppm) 33.3. Anal. Calcd (%) for $\text{C}_{40}\text{H}_{48}\text{B}_2\text{N}_3\text{Si}_2\text{Y}$: C, 65.14; H, 6.56; N, 5.70. Found: C, 64.68; H, 7.12; N, 5.80.

Reaction of $[(\text{C}_5\text{H}_5\text{BCH}_3)_2\text{YCl}]_2$ (3) with $\text{KN}(\text{SiMe}_3)_2$. The ^1H NMR investigation procedure is similar to that for $[(\text{C}_5\text{H}_5\text{BNET}_2)_2\text{YCl}]_2$, but with $[(\text{C}_5\text{H}_5\text{BCH}_3)_2\text{YCl}]_2$. $\text{K}[\text{C}_5\text{H}_5\text{BCH}_3]$ (**8**)¹³ was prepared as follows: A solution of $\text{KN}(\text{SiMe}_3)_2$ (186 mg, 0.935 mmol) in 4 mL of toluene was added to **3** (95.5 mg, 0.156 mmol) in 2 mL of toluene at –30 °C with stirring. The reaction mixture was gradually warmed to room temperature and then

Table 2. Crystallographic Data and Refinement for **1**, **2**, and **6**

	1	2	6
formula	C ₃₆ H ₆₀ B ₄ Cl ₂ N ₄ Y ₂	C ₇₅ H ₆₈ B ₄ Cl ₂ N ₄ Y ₂	C ₄₀ H ₄₈ B ₂ N ₃ Si ₂ Y
fw	840.84	1317.29	737.52
color	yellow	yellow	yellow
cryst syst	orthorhombic	monoclinic	orthorhombic
space group	<i>Ibca</i>	<i>Pn</i>	<i>P2(1)2(1)2(1)</i>
<i>a</i> , Å	8.7156(12)	11.8415(11)	8.6743(9)
<i>b</i> , Å	29.666(5)	11.8468(11)	17.8926(19)
<i>c</i> , Å	32.126(5)	24.244(2)	25.385(3)
α, deg	90	90	90
β, deg	90	101.164(2)	90
γ, deg	90	90	90
<i>V</i> , Å ³	8307(2)	3336.7(5)	3939.9(7)
<i>Z</i>	8	2	4
<i>D</i> _{calcd} , g/cm ³	1.345	1.311	1.243
<i>F</i> (000)	3488	1356	1544
θ range, deg	1.87 to 27.00	1.71 to 27.00	1.97 to 26.99
no. of reflns collected	22 779	19 412	23 361
no. of unique reflns	4535	9587	8529
no. of obsd reflns (<i>I</i> > 2σ(<i>I</i>))	1933	5145	3003
no. of params	222	787	439
final <i>R</i> , <i>R</i> _w (<i>I</i> > 2σ(<i>I</i>))	0.0431, 0.0821	0.0426, 0.0785	0.0487, 0.0707
Δρ _{max,min} , e Å ⁻³	0.434, -0.427	0.426, -0.513	0.309, -0.264

concentrated to approximately 1 mL to give a pale orange precipitate. The latter was separated, washed by 3 × 2 mL of toluene/hexane (v/v = 1:1), and extracted with 3 mL of THF. Evaporation of the yellow extract in vacuo gave a yellow solid, which was washed by 3 × 2 mL of hexane to provide **8** as a pale yellow solid (40 mg, 49% yield). ¹H NMR (300 MHz, C₆D₆, 25 °C): δ (ppm) 7.21 (dd, *J* = 10.2 Hz, *J* = 6.6 Hz, 2H, 3-/5-*H*), 6.59 (d, *J* = 10.2 Hz, 2H, 2-/6-*H*), 6.17 (t, *J* = 6.6 Hz, 1H, 4-*H*), 1.07 (s, 3H, CH₃). ¹H NMR (300 MHz, THF-*d*₈, 25 °C): δ (ppm) 6.97 (dd, *J* = 9.9 Hz, *J* = 7.2 Hz, 2H, 3-/5-*H*), 6.18 (d, *J* = 9.9 Hz, 2H, 2-/6-*H*), 5.90 (t, *J* = 6.9 Hz, 1H, 4-*H*), 0.42 (s, 3H, C H₃). ¹³C NMR (75 MHz, THF-*d*₈, 25 °C): δ (ppm) 133.6 (3-/5-*C*), 128.0 (2-/6-*C*), 109.4 (4-*C*), 4.7 (CH₃). ¹¹B NMR (128 MHz, THF-*d*₈, 25 °C): δ (ppm) 36.6.

Synthesis of (C₅H₅BCH₃)₂YN(SiMe₃)₂ (7**).** A solution of KN(SiMe₃)₂ (48.2 mg, 0.242 mmol) in 1.5 mL of toluene was added to **3** (74 mg, 0.121 mmol) in 2 mL of toluene at -65 °C with stirring. The reaction mixture was gradually warmed to room temperature. The reaction mixture was filtered, and evaporation of the yellow solution in vacuo gave an orange oil. The oil was extracted by 3 × 1.5 mL of hexane, the extract was concentrated to approximately 1 mL, and the residue was stored at -30 °C overnight. Some white precipitate that had formed was removed. Removal of the solvent gave **7** as a yellow oil (70 mg, 67% yield). ¹H NMR (400 MHz, C₆D₆): δ 7.24 (dd, *J* = 10.4 Hz, *J* = 7.2 Hz, 4H, 3-/5-*H*), 6.83 (d, *J* = 8.8 Hz, 4H, 2-/6-*H*), 6.18 (t, *J* = 7.2 Hz, 2H, 4-*H*), 1.03 (s, 6H, CH₃), 0.05 (s, 18H, Si(CH₃)₃). ¹³C NMR (100 MHz, C₆D₆): δ 140.1 (3-/5-*C*), 134.9 (2-/6-*C*), 112.8 (4-*C*), 5.9 (CH₃), 3.2 (Si(CH₃)₃). ¹¹B NMR (128 MHz, C₆D₆): δ 45.4. A satisfactory elemental analysis result for **7** could not be obtained. There are small amount of impurities, which show some signals at 0–0.4 ppm in ¹H NMR spectrum. As **7** is an oil, the impurities

could not be removed by recrystallization. The NMR (¹H, ¹³C, ¹¹B) spectra of the complex are provided as Supporting Information.

Intramolecular Hydroamination Catalyzed by the Boratabenzene Y Amides. The boratabenzene Y amide (**4**, **6**, or **7**), 2,2-dimethyl-1-aminopent-4-ene, and the standard *p*-xylene were mixed in C₆D₆ and transferred into a NMR tube. The NMR tube was heated at 90 °C, and the process of the reaction was monitored by ¹H NMR.

X-ray Crystallography. Suitable single crystals of **1**, **2**, and **6** were sealed in thin-walled glass capillaries, and data collection was performed at 20 °C on a Bruker SMART diffractometer with graphite-monochromated Mo Kα radiation (λ = 0.71073 Å). The SMART program package was used to determine the unit-cell parameters. The absorption correction was applied using SADABS. The structures were solved by direct methods and refined on *F*² by full-matrix least-squares techniques with anisotropic thermal parameters for non-hydrogen atoms. Hydrogen atoms were placed at calculated positions and were included in the structure calculation without further refinement of the parameters. All calculations were carried out using the SHELXS-97 program. Crystallographic data and refinement for **1**, **2**, and **6** are listed in Table 2.

Acknowledgment. This work was supported by the National Natural Science Foundation of China (Grant No 20672134) and Chinese Academy of Sciences.

Supporting Information Available: NMR (¹H, ¹³C, ¹¹B) spectra of the lithium and potassium salts of boratabenzene anions and **7**; CIF files giving X-ray crystallographic data for **1**, **2**, and **6**. This material is available free of charge via the Internet at <http://pubs.acs.org>.

OM800770A